86-02665/

NATIONAL AERONAUTICAL ESTABLISHMENT

SCIENTIFIC AND TECHNICAL PUBLICATIONS

AERONAUTICAL REPORTS:

Aeronautical Reports (LR): Scientific and technical information pertaining to aeronautics considered important, complete, and a lasting contribution to existing knowledge.

Mechanical Engineering Reports (MS): Scientific and technical information pertaining to investigations outside aeronautics considered important, complete, and a lasting contribution to existing knowledge.

AERONAUTICAL NOTES (AN): Information less broad in scope but nevertheless of importance as a contribution to existing knowledge.

LABORATORY TECHNICAL REPORTS (LTR): Information receiving limited distribution because of preliminary data, security classification, proprietary, or other reasons.

Details on the availability of these publications may be obtained from:

Publications Section,
National Research Council Canada,
National Aeronautical Establishment,
Bldg. M-16, Room 204,
Montreal Road,
Ottawa, Ontario
K1A 0R6

ÉTABLISSEMENT AÉRONAUTIQUE NATIONAL

PUBLICATIONS SCIENTIFIQUES ET TECHNIQUES

RAPPORTS D'AÉRONAUTIQUE

Rapports d'aéronautique (LR): Informations scientifiques et techniques touchant l'aéronautique jugées importantes, complètes et durables en termes de contribution aux connaissances actuelles.

Rapports de génie mécanique (MS): Informations scientifiques et techniques sur la recherche externe à l'aéronautique jugées importantes, complètes et durables en termes de contribution aux connaissances actuelles.

CAHIERS D'AÉRONAUTIQUE (AN): Informations de moindre portée mais importantes en termes d'accroissement des connaissances.

RAPPORTS TECHNIQUES DE LABORATOIRE (LTR): Informations peu disséminées pour des raisons d'usage secret, de droit de propriété ou autres ou parce qu'elles constituent des données préliminaires.

Les publications ci-dessus peuvent être obtenues à l'adresse suivante:

Section des publications
Conseil national de recherches Canada
Établissement aéronautique national
Im. M-16, pièce 204
Chemin de Montréal
Ottawa (Ontario)
K1A 0R6

UNLIMITED
UNCLASSIFIED

HIGH TEMPERATURE OXIDATION AND HOT CORROSION OF NICKEL AND COBALT BASED SUPERALLOYS

OXYDATION À HAUTE TEMPÉRATURE ET CORROSION À CHAUD DES SUPERALLIAGES À BASE DE NICKEL ET DE COBALT

by/par

P.C. Patnaik

National Aeronautical Establishment

AERONAUTICAL NOTE
NAE-AN-33
NRC NO. 25075

OTTAWA
OCTOBER 1985

W. Wallace, Head/Chef
Structures and Materials Laboratory/
Laboratoire des structures et matériaux

G.M. Lindberg
Director/Directeur

ABSTRACT

Oxidation and hot corrosion are often the two most important modes of degradation that superalloys undergo in a high temperature gas turbine atmosphere. In general, the corrosion resistance of superalloys has been sacrificed to achieve adequate high temperature strength. Therefore turbine blade and vane materials are often protected from these modes of degradation by the use of protective coatings. Three classes of coating materials based on aluminizing, chromizing and more recently siliconizing treatments are usually considered due to their resistance to oxidation, sulfidation (hot corrosion) processes.

The purpose of this paper is to review the oxidation and hot corrosion properties of superalloys and coating materials of relevance to aero gas turbine engine hot-section, with particular emphasis on the interaction between gas phase or molten salt deposits and the substrate alloy/coating system. The recent theories on these processes are reviewed. Finally, the effects of erosion on the corrosion properties of superalloys and coatings are also discussed.

RÉSUMÉ

L'oxidation et la corrosion à chaud sont dans bien des cas les deux modes d'endommagement les plus importants que subissent les superalliages dans les gaz chauds d'une turbine à gaz. D'une façon générale, la résistance de ces alliages à ce type d'endommagement est sacrifiée à leur resistance au fluage. Leur utilisation pour aube de rotor ou aube directionnelle nécessite donc dans la plupart des cas l'emploi d'un revêtement protecteur. Il existe trois classes de revêtement pour superalliage contre l'oxidation et la sulfidation (corrosion à chaud) que l'on obtient par aluminage, chromisation ou siliciumisation de la surface de l'alliage.

On résume dans cet article les propriétés d'oxidation et de corrosion de superalliages et de revêtements protecteurs pour composantes chaudes de turbines à gaz aéropropulsives. On met l'emphase sur les interactions entre phases gazeuses ou phases liquides de dépôts salins et l'alliage et son revêtement. On donne ensuite un aperçu des théories émises sur les modes d'endommagement. On discute enfin des effets de l'érosion sur la corrosion des alliages et de leurs revêtements.

CONTENTS

		Page
	ABSTRACT	(iii)
	ILLUSTRATIONS	(v)
1.0	INTRODUCTION	1
2.0	OXIDATION	1
	2.1 Oxide Defect Structure	1
	2.2 Effect of Impurities (Doping)	3
	2.3 Growth of Protective Oxides	3
	2.4 Internal Oxidation	4
	2.5 Oxidation in Complex Atmospheres	4
	2.6 Oxide Adherence	5
3.0	HOT CORROSION	6
	3.1 Modes of Hot Corrosion	6
	3.2 Effect of Alloy Composition	7
	3.3 Effect of Temperature	8
	3.4 Mechanisms of Hot Corrosion	8
	3.4.1 Thermochemistry	8
	3.4.2 Fluxing Models	9
	3.5 Inhibition of Hot Corrosion	10
4.0	EROSION AND CORROSION	10
5.0	CONCLUSIONS	11
6.0	ACKNOWLEDGEMENTS	12
7.0	REFERENCES	12

TABLES

Table		Page
1	Parabolic Rate Constants* for Sulfidation and Oxidation of Some Binary and Ternary Alloys	19
2	Composition of Sea Water	19
3	Relative Ranking Order of Oxides Which Lower O^{2-} Content of Na_2SO_4 (Calculated at 1200K)	20

ILLUSTRATIONS

Figure		Page
1	Temperature Dependence of the Parabolic Rate Constants for the Growth of Various Oxide Barriers on Pure Metals	21
2	Oxide Map for Ni-Cr-Al System	22
3	Isothermal Section at 1273K in the Ni-Al-O Phase Diagram	23
4	Stability Diagram for Ni-S-O System as a Function of Temperature	24
5	Stability Diagram for Ni-S-O at 1200K	24
6	Hot Corrosion Cronology	25
7	Stability Diagram Showing the Phases of Aluminum that are Stable in Na_2SO_4 at 1273K	26
8	Stability Diagram Showing the Displacement of the Boundary (Arrows) at Which Acidic Fluxing of Al_2O_3 Can Occur	27
9	Alloy Systems Susceptible to Attack by Hot Corrosion and Procedures to Inhibit Such Degradation	28
10	Kinetics Data from the Testing of Materials at 1144K in the Oxidation-Erosion Test	29
11	Kinetics Data for Materials Exposed to Erosion-Hot Corrosion Conditions	30

HIGH TEMPERATURE OXIDATION AND HOT CORROSION OF NICKEL AND COBALT BASED SUPERALLOYS

1.0 INTRODUCTION

Nickel and cobalt based superalloys containing about 20 w/o Cr generally maintain adequate high temperature strength as well as oxidation and corrosion resistance at temperatures up to ~1173K. However, with the increasingly demanding requirements of modern aircraft gas turbines, stronger alloys are needed to operate beyond this limit. In practice this has been achieved by reducing the chromium content to about 10 w/o to permit an increased amount of γ' hardening. This is done however at the expense of high temperature oxidation resistance and perhaps more importantly, at the expense of hot corrosion resistance. Therefore to protect the materials from oxidation and hot corrosion, various types of coatings based on aluminum, chromium and more recently silicon have been used[1]. The oxide layer on the aluminide type of coatings although good for oxidation, does not provide adequate protection for hot corrosion. On the other hand, Cr_2O_3 on chromium based coatings has been successful in protecting the materials from hot corrosion, but the application of these coatings has been limited to ~1223K due to the volatilization of Cr_2O_3. Meanwhile little is known about the silicon based coatings and is the subject of extensive current investigations. The purpose of this paper is to discuss the basic protection mechanisms of aluminum, chromium and to a lesser extent of silicon oxides on coatings as well as on substrates of interest to aero gas turbine engine applications in oxidizing, sulfidizing and corroding-eroding atmospheres.

2.0 OXIDATION

The formation of an oxide layer on an alloy or coating, if chemically and mechanically stable, acts as a barrier between the material and the gaseous environment. Further growth of this layer becomes limited if the transport of reacting species through the oxide layer is rate controlling. Oxide reaction products are usually thermodynamically more favourable because of the greater affinity of most metallic elements for oxygen as compared to other oxidants such as sulfur[2] and nitrogen[3].

Oxide barriers are generally more effective in inhibiting reactions between alloys and various environments than other type of barriers such as sulfides. This is due to the fact that sulfide structures possess a considerable degree of disorder (high non-stoichiometry) and high dissociation pressures compared to corresponding oxides. In addition, the eutectic temperatures for metal-sulfide systems are considerably lower than eutectic temperatures for corresponding metal-oxide systems[4]. Therefore, catastrophic corrosion caused by the formation of liquid corrosion products, appears in sulfur containing environments at lower temperatures than in pure oxygen atmosphere. These facts are evident upon comparing the parabolic rate constants for growth of oxides and sulfides (Table I).

Among the oxide barriers it is seen from Figure 1 that Al_2O_3, SiO_2 and Cr_2O_3 are the most effective barriers to oxidation, respectively in a decreasing order. Possibilities also exist to decrease the growth rates of Al_2O_3, SiO_2 and Cr_2O_3 barriers further and make them mechanically more stable by the addition of minor alloying elements. In the following, the oxide defect structure, the effect of impurities and doping, oxide growth structure and internal oxidation relevant to nickel and cobalt based superalloys and various coating systems are discussed.

2.1 Oxide Defect Structure

Unlike stoichiometric ionic crystals (such as NaCl or AgBr) which show predominantly ionic defects, oxides formed as a result of oxidation of alloys are generally non-stoichiometric and therefore exhibit both ionic and electronic conductivity. In the oxide, the type of defects on the anion and cation sublattices are respectively oxygen vacancies (V_o) and interstitials (O_i), metal vacancies (V_M) and interstitials (M_i). The electronic defects are either free electrons e or free holes h.

To maintain electrical neutrality, these defects effectively carry an electrical charge such as negative (a dash ′) or positive (a dot •). In any type of oxide only one of these defects may be predominant although other defects may be present. There are two types of non-stoichiometric oxides. The typical equations governing the formation of point defects in these type of oxides are as follows. In these equations, M_M and O_o represent metal in a metal sublattice and oxygen in an oxygen sublattice with x and y as the non-stoichiometry in respective sublattices.

I. p-type oxides, $M_{1-x}O$ (metal deficit) and MO_{1+y} (excess oxygen)

II. n—type oxides, $M_{1+x}O$ (metal excess) and MO_{1-y} (oxygen deficit)

(a) Metal Deficit

$$1/2O_2 \rightleftharpoons V_M'' + 2h^{\bullet} + O_o \qquad (1)$$

Eg. NiO, FeO, CoO, Cu_2O, MnO, Mn_3O_4, Cr_2O_3, $CoAl_2O_4$, $NiAl_2O_4$ and $FeCr_2O_4$

(b) Excess Oxygen

$$1/2O_2 \rightleftharpoons O_i'' + 2h^{\bullet} \qquad (2)$$

Eg. Fe_2O_3, Al_2O_3 generally at very high oxygen pressure.

(c) Metal Excess

$$1/2O_2 + M_i^{\bullet\bullet} + 2e' \rightleftharpoons M_M + O_o \qquad (3)$$

Eg. ZnO, CdO, PtO, Ag_2O, Al_2O_3

(d) Oxygen Deficit

$$1/2O_2 + V_o^{\bullet\bullet} + 2e' \rightleftharpoons O_o \qquad (4)$$

Eg. TiO_2, HfO_2, ZrO_2 and oxides of Nb, Ta and W.

In the majority of p-type oxides, the predominant growth process takes place by the movement of cations through diffusion by vacancies and therefore new oxide forms at the gas/oxide interface. In the case where the predominant process is the movement of anions, new oxide forms at the scale/metal interface. In the former case, the rate of growth of oxide layers such as NiO, CoO and FeO have been calculated assuming a lattice diffusion controlled process and good agreement between theory and experiment have been achieved[7-9]. Since the levels of non-stoichiometry in these transition metal oxides are quite high (x ranging from 10^{-2} to 0.15 in $M_{1-x}O$), more refinement of the defect structure of these oxides taking into account the defect clustering and defect/defect interaction has resulted in excellent agreement between calculated and experimental results[10]. Using a similar approach, far less success has been achieved for oxides such as Al_2O_3 and Cr_2O_3 of technological importance because of additional factors such as recrystallization, convoluted scale growth and oxide ridge development[11-14].

The oxides Al_2O_3 and Cr_2O_3 are the only ones thermodynamically stable respectively in Al-O and Cr-O systems. Corundum (α-Al_2O_3), stable at temperatures exceeding 1223K[15] and Cr_2O_3 have an identical crystal structure consisting of a hexagonal close-packing of oxygen ions with the trivalent cations occupying two-thirds of the octahedral interstices[16]. Oxygen migration in Cr_2O_3

single crystal is about three orders of magnitude slower than Cr suggesting predominant cation disorder with Cr_i^{Z+} interstitials. In Al_2O_3, both Al and O are mobile and diffuse approximately at the same rate in the grain boundary of polycrystalline specimens. Bulk self-diffusion of oxygen is much slower than that of Al. Predominant oxygen transport in the Al_2O_3 scale on an active-element containing alloy (FeCrAlY) has been observed[17]. SiO_2 on the other hand has been observed to conduct predominantly oxygen interstitial ions. A detailed review of the defect and transport properties of these three oxides can be found in recent literature[14,18].

2.2 Effect of Impurities (Doping)

The concentration of point defects in a semi-conducting oxide is affected by doping. In a p-type semi-conductor, if the dopant has a valency higher than that of the host ion then the point defect concentration will increase in order to maintain a charge neutrality. For example doping Al^{3+} ions into $Ni_{1-x}O$ will result in an increase in the nickel vacancy (V''_{Ni}) concentration[19] such that:

$$Al_2O_3 = 2\,Al^{\bullet}_{Ni} + V''_{Ni} + 3\,O_o \qquad (5)$$

A similar result can be expected by doping chromium into $Ni_{1-x}O$. In contrast, when a lower valent ion such as Li^+ is doped into $Ni_{1-x}O$ then a corresponding decrease in nickel vacancy concentration is observed[20].

$$Li_2O + 1/2O_2 = 2\,Li'_{Ni} + 2h^{\bullet} + 2\,O_o \qquad (6a)$$

and

$$Li_2O + V''_{Ni} = 2\,Li'_{Ni} + O_o \qquad (6b)$$

In the oxidation of alloys, doping effects in oxides are generally detectable at concentrations of the additive in the alloy of about 0.1%. The effect of doping becomes insignificant as the non-stoichiometry of the host oxide increases[21]. It should be noted that for the dopant to be effective the dopant oxide should be thermodynamically more stable than the host oxide. This is why more reactive or stable oxides (eg. Y_2O_3 or Hf_2O_3) must be considered for doping technologically more important oxides such as Al_2O_3 and Cr_2O_3.

2.3 Growth of Protective Oxides

Among the three oxides Al_2O_3, Cr_2O_3 and SiO_2 it is well established that the first two provide very good oxidation protection when formed on alloys or coatings. A typical oxide map for the Ni-Cr-Al system displaying the alloy and coating composition is shown in Figure 2 depicting the composition range over which Al_2O_3, Cr_2O_3 and NiO predominate[14]. At temperatures in the range of 1173 to 1473K, Al_2O_3 scale appears to provide a greater protection than Cr_2O_3 because the diffusion rates of species in Al_2O_3 are much slower than in Cr_2O_3. Protective properties of Cr_2O_3 are reduced at temperatures above 1223K and a high flow rate of gas in oxidizing atmospheres[22-24] because of the accelerated oxidation of Cr_2O_3 to volatile CrO_3 under such conditions. Also Cr_2O_3 will transform to volatile $Cr(OH)_3$[25] in the presence of water vapour at these temperatures. Since the free energy of formation of Al_2O_3 is appreciably greater than that of chromia[8], internal oxidation of aluminum will occur where the protective scale is chromia (eg. IN-738). Internal oxidation causes a loss of the alloying aluminum content and may be detrimental to the high temperature strength of the superalloy. SiO_2 has been used as a protective oxide on silicide coating, but elevated temperature reduction of SiO_2 to SiO does occur in reducing atmospheres. Also there is some evidence that SiO_2 can react with other metallic ions to form complex molten oxides[25].

In most situations alloys and coatings do not contain enough of the element (eg. Al, Cr and Si) whose oxide is the most thermodynamically stable to permit the alloy surface, to become totally covered with this oxide. Therefore, less stable oxides of the base metal are formed (NiO and CoO in the case of nickel and cobalt based superalloys). The oxidation theory for this type of process has been developed by Wagner[26-29], Rapp[30,31], Kirkaldy[32] and Smeltzer[33]. More recent analyses of these processes with emphasis on the diffusional as well as thermodynamic aspects have led to further refinement of this theory[34,35]. These theories have been recently reviewed by the author[36]. The theories behind the short-circuit and related transport processes with reference to oxides of Ni, Cr, Si and Al have also been reviewed adequately elsewhere[37].

2.4 Internal Oxidation

Internal oxidation of alloys is held to occur through dissolution of atomic oxygen into the base metal at its surface (in the absence of a scale) or at the metal-scale interface. The dissolved oxygen diffuses inwards through the metal matrix containing some previously precipitated internal oxide particles. Inward diffusion of oxygen and outward diffusion of the alloying element continuously provide oxygen and alloying element concentrations in excess of those corresponding to the solubility product of the alloying element oxide. The conditions necessary for the occurrence of internal oxidation in an alloy has been summarized in Reference 31.

A typical isothermal section (1273K) in the Ni-Al-O phase diagram is shown in Figure 3. Similar data are also available for Ni-Cr-O isothermal section[39]. Thermodynamic calculations have shown that Al_2O_3 and Cr_2O_3 are stable in contact with alloys containing trace or very small amounts of Al and Cr respectively[40,41]. Although stable over virtually the entire alloy composition range, whether these oxide phases are able to form as internal oxides or continuous oxide layers depends on factors such as relative diffusion rates in the alloy and the scale[26,42], the alloy bulk composition and oxygen potential in the gas phase. For nickel and cobalt based superalloys according to these analyses, the minimum solute concentration to avoid internal oxidation and establish a continuous oxide layer is around 15–25 wt. % Cr and 4 to 6 wt. % Al in oxygen at atmospheric pressure.

If the prior information such as oxygen solubility and diffusivity, alloying element diffusivity, alloy composition and its thermodynamics and stability of the oxides are known, one can predict the oxide microstructure in relatively simple binary alloys by superimposing the diffusion path on a ternary isotherm[34,43]. This has been achieved with success in nickel based alloys[44]. More complication would arise in multicomponent alloy systems such as nickel based IN-713C, IN-738C or MAR-M246 in terms of the complexities in their microstructure, thermodynamics and diffusional properties.

2.5 Oxidation in Complex Atmospheres

The gas turbine atmosphere is usually complex containing several oxidants such as S_2 and N_2 other than oxygen of which reaction due to sulfur is very aggressive. Therefore, oxidation behaviour of a metal or an alloy in a multi-oxidant environment differs considerably than in pure oxygen. For example in a simple situation when pure nickel is subjected to a mixed atmosphere containing sulfur as well as oxygen (Ni-S-O), the following reactions can take place[45].

$$Ni + 1/2O_2 = NiO \quad (7)$$

$$NiS + 2O_2 = NiSO_4 \quad (8)$$

$$3Ni + S_2 = Ni_3S_2 \quad (9)$$

$$Ni_3S_2 + 1/2S_2 = 3NiS \quad (10)$$

$$2Ni + S_2 = 2NiS \quad (11)$$

$$Ni_3S_2 + 3/2O_2 = 3NiO + S_2 \quad (12)$$

$$2NiS + O_2 = 2NiO + S_2 \quad (13)$$

$$2NiSO_4 = 2NiO + S_2 + 3O_2 \quad (14)$$

$$4NiO + Ni_3S_2 = 7Ni + S_2 + 2O_2 \quad (15)$$

$$2NiO + 7NiS = 3Ni_3S_2 + 1/2S_2 + 2O_2 \quad (16)$$

$$3NiSO_4 + NiS = 4NiO + 2S_2 + 4O_2 \quad (17)$$

A schematic representation of these equilibria (Eqns. 7 through 17) is shown in Figure 4 as a function of temperature and partial pressures of oxygen and sulfur. In this figure the stability region for a single condensed phase appears as a volume, two condensed phases as a plane (Eqns. 7 to 14) and three condensed phases as a line (Eqns. 15 to 17). Often, for ease of representation, two dimensional sections are made perpendicular to one of the axes, particularly at constant temperature (Fig. 5). For simplicity, these diagrams have been constructed at unit activity of the reactants. From this example, one can appreciate the complexity that would arise in a situation when a multi-component alloy with different alloying element activities equilibrates with the gas mixture. Inspite of these difficulties, attack of some alloys in complex multicomponent atmospheres have been understood at least qualitatively[46-48]. Mechanisms by which these complex interactions occur have been proposed but not all the parameters necessary to allow the calculation of reaction rates and component lives are available.

When the environment consists of a liquid deposit such as Na_2SO_4 (in hot corrosion), the effects of various components in the liquid can be considered in the same way as those described above for the gaseous environment. An additional undesirable feature however is that any oxide if produced in this complex environment, may react or dissolve in the liquid deposit. A detailed discussion of the mechanism of these processes follow in a subsequent section.

2.6 Oxide Adherence

The protection of alloys or coatings from the complex corrosive atmosphere is reduced at high temperature if the oxide reaction products spall due to the scale growth processes and thermally induced stresses under cyclic conditions. The adhesion of oxide barriers to the alloys or coatings is therefore of critical importance. The most important mechanistic models explaining the improved scale adherence such as: (a) enhanced scale plasticity, (b) modification to scale growth process, (c) chemical bonding, (d) vacancy sink model, and (e) oxide pegging have been discussed in detail elsewhere[49]. Of these mechanisms, the elimination of interfacial voids and the oxide peg formation seem to be of most significance in many cases. The formation of oxide pegs has been considered as the decisive factor in oxide adhesion during the later stages of growth, whereas vacancy sink processes have been considered important in the early stages. Co-Cr-Al alloys containing 1 wt. % of Ce or Y or Hf have been observed to have improved Al_2O_3 scale adhesion by the growth of Al_2O_3 oxide intrusions into the alloy around the internal oxide particles of these rare earth elements[50,51].

3.0 HOT CORROSION

Hot corrosion is a form of accelerated oxidation (or sulfidation) of alloys which occurs in high temperature combustion gases in the presence of certain impurities. In general, in the gas turbine engine applications, hot corrosion problems are associated with the presence of molten vanadium (from the fuel) or sodium sulfate compounds from the marine or salt atmospheres (Table II). Depending on the purity of the fuel, it can also act as a source of salt even in the absence of a salt atmosphere when impurities such as Na, Pb and V are present. Sulfates for instance can be formed directly during combustion due to the reaction between these metallic impurities and the sulfur in the fuel. However, in most situations, introduction of salts like Na_2SO_4 or NaCl from the atmosphere causes the most serious problem in the turbines.

Molten sodium sulfate ($T_m \sim 1157K$), the principal agent in promoting sulfidation is formed as follows:

$$\underset{\text{(from sea salt)}}{2NaCl} + \underset{\text{(from fuel)}}{S} + \underset{\text{(from air)}}{2O_2} = Na_2SO_4 + Cl_2 \qquad (18)$$

Once the alloy surface has been partially or completely covered by the molten salt, conditions for severe corrosion develop. The kinetics of sulfate induced hot corrosion and the morphology of the corrosion products can vary considerably. For a given set of exposure conditions, the rate of attack of different alloys can differ by more than three orders of magnitude. For a given alloy the corrosion rate depends on several variables such as composition and velocity of the atmosphere, composition of the salt deposit and its thickness, rate of salt deposition, temperature, thermal cycling and more importantly the time[52]. A detailed discussion of these topics is outside the scope of this paper. For an excellent presentation of these topics and more, the reader is referred to several review articles[51-57].

3.1 Modes of Hot Corrosion

Hot corrosion of virtually all susceptible alloys is observed to occur in two stages.

a. An initiation stage.

b. A propagation stage.

In the initiation stage the alloy is oxidized to produce a reaction product barrier usually Al_2O_3 or Cr_2O_3, with sulfides forming in the alloy due to sulfur penetration in the scale. This process gives rise to a depletion of the alloying elements (Al or Cr) from the alloy surface. Other processes that take place in this stage include the development of growth stresses in the oxide and dissolution of oxides in the salt deposit. The chemical changes due to these processes can result in shifts in salt composition towards more corrosive conditions. The length of this stage varies from seconds to thousands of hours and depends on a large number of variables as shown in Figure 6. The end of the initiation stage occurs when local penetration of the salt through the scale reaches the low oxygen activity scale-alloy interface. This situation leads to the rapid propagation stage. The best means to avoid or minimize hot corrosion attack is to have alloys or coatings that remain in the initiation stage as long as possible.

The propagation stage is accompanied by very severe attack of the alloy. The relationship between the initiation and propagation stages is also indicated schematically in Figure 6. The degradation modes have been generally classified into two types one of which involves fluxing reactions where the oxide scales formed on alloys or coatings can react with the liquid deposit. Sodium sulfate (Na_2SO_4) may be considered to be composed of a basic component Na_2O (or O^{2-} ions) and an acid component (SO_3). In a liquid Na_2SO_4 deposit the sulfate ion decomposes according to the reaction

$$SO_4^{2-} = 1/2O_2 + SO_2 + O^{2-} \qquad (19)$$

The sodium sulfate melt therefore has an oxygen ion or Na_2O activity which is defined by the oxygen and SO_2 potentials. In terms of this chemistry two types of salt fluxing mechanism exist.

I. **BASIC FLUXING**; in which the oxide scale on the alloy or coating reacts with Na_2O and dissolves in the salt as anionic species.

$$MO + O^{2-} = MO_2^{2-} \tag{20}$$

If the oxygen ion activity of the sulfate melt is high compared to that required to form complex ions such as MO_2^{2-} in the above reaction, then the metal oxide (MO) dissolves in the melt as a complex anion.

II. **ACIDIC FLUXING**; in which the oxygen ion concentration of the melt is low compared to the value required to maintain equilibrium in the dissociation reaction of the metal oxide according to

$$MO = M^{2+} + O^{2-} \tag{21}$$

Consequently the metal oxide simply dissolves in the melt.

When both the acidic and basic fluxing equations are combined it is apparent that the concentration of the metal M in the melt would go through a minimum as a function of oxide ion activity. The increase in solubility of metal with increasing Na_2O activity (decrease in p_{SO_3}) corresponds to basic fluxing whereas the increase in solubility of metal with decreasing Na_2O activity corresponds to acidic fluxing. The terms acid and basic are relative and refer to the reactions that occur rather than to just the condition of the melt. For example, the conditions for acidic fluxing of one oxide could equally cause basic fluxing of another oxide because of the difference in stabilities of various complex anions and interactive dissolution[52].

3.2 Effect of Alloy Composition

Detailed correlations between the alloy compositions and their hot corrosion resistances have been published[58-61] and reviewed by Stringer[53]. There is general agreement that the most important alloying constituent providing protection against hot corrosion is chromium. Considerable disagreement exists about the effects of other elements although the majority view is that molybdenum is harmful. According to Stringer[53], there is a critical amount of Mo above which severe corrosion is induced by Mo in aggressive environments; the critical amount probably increases with increasing chromium content, at least for Cr_2O_3-forming alloys; the value is approximately 4-5 wt. % Mo for 15 wt. % Cr alloys, rising perhaps to 10 wt. % Mo for 25% Cr alloys. For superalloys like MAR-M 246 with about 9% Cr, Mo contents of 2 to 3% may still be harmful. High carbon contents are harmful in the presence of Mo, since they may result in large Mo-rich carbide particles which can encourage local catastrophic fluxing of the protective scale. Tungsten behaves like Mo but appears to be less harmful. Rare earths like Ce and La in metallic form do little or no good although beneficial effects has been obtained by adding rare earth oxides such as CeO_2, La_2O_3 into the sulfate melt. The oxides act by getting the sulfur to form stable oxysulfides of the form M_2O_2S[63].

In Al_2O_3-forming alloys the situation is different. Increasing Cr contents continues to be beneficial and this effect is related to the capacity of the system to reheal after any scale breakdown. Molybdenum seems to be harmful but depends quite sensitively on how severe the corrosive environment is.

Cobalt based superalloys are generally regarded as having better corrosion resistance than those based on nickel, but this may be due to the higher Cr content of most cobalt based superalloys (eg. 25 wt. % Cr in X-40). In severe sulfidation conditions cobalt based superalloys are better[62]

because of a high cobalt/cobalt sulfide eutectic (m.p. 1153K) than the nickel/nickel sulfide eutectic (m.p. 918K). For an excellent review on the effects of alloying elements on hot corrosion of superalloys, the reader is referred to an article by Davin and Coutsouradis[64]. Hot corrosion of cobalt based superalloys has been described recently by Luthra[65].

3.3 Effect of Temperature

In general, the effect of temperature on hot corrosion in practical gas turbine situations cannot clearly be assessed from service experiences. In some aviation and marine engines, the region of severe attack is near the mid-section airfoils of blades or vanes. In others it affects normally the shroud or the root platform. This can be rationalized however, since it is well established that blades and vanes are subjected in service to large temperature gradients along their longitudinal directions. On the other hand, the severity of sulfidation is known to increase with an increase in temperature up to a maximum beyond which it starts to decrease due to the volatilization of the molten sulfates. In other words, there is an intermediate temperature at which sulfidation damage can be expected to be maximum. In some applications these may correspond to mid airfoil temperature while in others it may correspond to shroud or root platform temperatures. Therefore, not surprisingly, maximum damage can occur at mid airfoil or at its extremities and this depends on the particular engine design parameters and its operating conditions.

It should be emphasized that while severe hot corrosion effects occur only in a certain temperature range in which sodium sulfate condenses in a molten form, other forms of corrosion that differs in the mechanism involved can occur above and below this range. Under service conditions the temperatures at which Na_2SO_4 either melts or vapourizes can be expected to drop depending on the composition of the modified deposit due to the formation of a Na_2SO_4-NaCl eutectic or by the formation of a complex salt. This drop in temperature increases the range in which the alloys or coatings are generally subjected to hot corrosion.

3.4 Mechanisms of Hot Corrosion

3.4.1 Thermochemistry

The chemistry of hot corrosion process was first described by Simons et al.[67]. In their studies they distinguished two stages: (i) a triggering stage associated with the initial reduction of sodium sulfate, the reducing agent R being usually the alloy, but pyrolytic carbon resulting from poor combustion of the fuel may also act as a reducing agent sometimes.

$$Na_2SO_4 + 3R = Na_2O + 3RO + S \qquad (22)$$

The sulfur released by this reaction sulfidizes the metal

$$M + S = MS \qquad (23)$$

In the second stage (ii) a rapid "auto catalytic" destruction reaction occurs.

$$Na_2SO_4 + 3MS = 4S + 3MO + Na_2O \qquad (24)$$

and

$$4M + 4S = 4MS$$

3.4.2 Fluxing Models

The fluxing model for hot corrosion was first proposed by Decrescente and Bornstein[68] and later improved by several workers[69-72]. All models are based on phase stabilities and how these are affected by compositional change of the molten deposit as a result of oxidation and sulfidation. Since most of the superalloys contain Al for high temperature oxidation resistance, consideration of the Al-O-S phase diagram in the region of Na_2SO_4 indicates that the stability of Al_2O_3 is a function of the acidity or basicity of the Na_2SO_4 as shown in Figure 7. This diagram has been constructed by calculating the equilibrium pressure from the following reactions[69].

$$Al_2O_3 + 3SO_3 = Al_2(SO_4)_3 \quad (25)$$

$$Al_2S_3 + 6O_2 = Al_2(SO_4)_3 \quad (26)$$

$$Al_2O_3 + 3SO_3 = Al_2S_3 + 6O_2 \quad (27)$$

$$Na_2SO_4 + Al_2O_3 = 2NaAlO_2 + SO_3 \quad (28)$$

To use this diagram, it is necessary to know the composition of the deposit. Unfortunately, even when the barrier is stable under the as-deposited condition, reactions can occur which cause the composition of the deposit to be changed such that the barrier is no longer stable. The cross (X) in Figure 7 indicates the approximate composition of the salt deposit in a gas turbine[69]. It can be seen that the Al_2O_3 barrier is thermodynamically stable in this deposit and will form as a layer between the Na_2SO_4 and the alloy. The formation of Al_2O_3 lowers the oxygen activity across the Na_2SO_4 and the composition of the Na_2SO_4 adjacent to the Al_2O_3 is changed as shown by the arrows in Figure 7. This reduction in oxygen activity causes the sulfur activity in Na_2SO_4 to become much greater than that in the gas phase. In addition, sulfur penetrates the Al_2O_3 barrier and forms sulfides underneath the Al_2O_3. Experimental results indicate that sulfur diffuses through Al_2O_3[70]. Evidence of sulfur diffusion through NiO and Cr_2O_3 under similar conditions has been published by Pettit et al.[47]. The reduction of sulfur activity underneath the Al_2O_3 again causes the oxide ion activity to be increased in the Na_2SO_4 to levels at which Al_2O_3 reacts with the O^{2-} ions to form aluminate ions thereby decreasing the protectiveness of Al_2O_3.

Similar reactions occur with chromium with the exception that Cr is effective in preventing basic fluxing reactions because Cr_2O_3 reacts with O^{2-} ions and prevents the activity of O^{2-} from reaching the levels required for basic fluxing. Moreover, although the O^{2-} activity is low, it is not low enough to cause acidic fluxing. In addition, Cr also inhibits the adverse effects produced by sulfur in some alloys by forming Cr sulfides thereby preventing the formation of other deleterious sulfide phases such as aluminum sulfide and nickel sulfides[69].

In considering the reaction of oxides with Na_2SO_4, it is necessary to consider the reactions between the protective oxides and other acidic components which are introduced into the modified Na_2SO_4 as a result of oxide contaminant. One such example is shown in Figure 8 where MoO_3 is introduced as a contaminant, and this is important since most of the superalloys contain molybdenum. Similar arguments would apply for contamination of Na_2SO_4 with V_2O_5 or WO_3 where the former oxide can be introduced into the Na_2SO_4 through the gas due to combustion of vanadium-containing fuel, whereas the latter oxide could be introduced into the Na_2SO_4 from the hot corrosion of an alloy containing tungsten (MAR-M 246 contains ~ 10 wt. % W). The reaction between MoO_3 and Na_2SO_4 shows that an obvious effect

$$MoO_3 + Na_2SO_4 = Na_2MoO_4 + SO_3 \quad (29)$$

of MoO_3 in Na_2SO_4 is to cause the equilibrium pressure of SO_3 in Na_2SO_4 to be increased. However, as shown in Figure 8 even when the activity of MoO_3 in Na_2SO_4 is unity, the SO_3 pressure is still not sufficient to cause reaction between SO_3 and Al_2O_3. But reaction between MoO_3 and Al_2O_3 in Na_2SO_4 occurs at an activity of $MoO_3 \simeq 0.1$ or greater and experimental evidence of this has been shown by Goebel et al.[69]. The reaction products in such cases (Mo, V and W) are either soluble in the modified Na_2SO_4 or in the liquid state. Consequently, the protective Al_2O_3 oxide layer is destroyed and its subsequent reformation is prevented. Although the interaction between protective oxides (Al_2O_3, Cr_2O_3 and SiO_2) and the low melting oxides such as MoO_3 and V_2O_5 are not well documented, their direct interaction with sodium sulfate is quite well established and summarized in Table III[71,72].

The role of silicon in hot corrosion atmospheres is not very well known and currently much of the research is in progress[73]. Some of the early research has shown that[71] SiO_2 formed as a result of oxidation of silicon, lowers the oxide ion content of the fused salt sufficiently so that deleterious reaction between oxide ions and the protective scale (Al_2O_3, Cr_2O_3) does not occur. However, sodium silicate $Na_2Si_2O_5$ (m.p. 1147K) formed as a result of reaction between SiO_2 and Na_2SO_4, reacts with the protective oxides to form a complex glass. When thermally shocked, this glass becomes non-protective possibly fracturing due to the difference in coefficients of thermal expansion between the "glass" and the metal substrate. In such situations, when reheated, the liquid Na_2SO_4 can come in contact with the substrate directly. Recent research has shown that siliconizing of superalloys has led to an improvement in oxidation and hot corrosion properties[74].

It is difficult to present a unique model for hot corrosion process since it depends on so many important variables (Fig. 6). Inspite of the fact that a wide range of corrosion rates and corrosion morphology are observed, quantitative models for fluxing have been presented by a number of workers. These models involving transport of various reacting species ie. M and O in the oxide coupled with the transport of oxidants and of dissolved oxide through the salt layer have recently been reviewed by Shores[52].

3.5 Inhibition of Hot Corrosion

The alloy systems which are susceptible to different types of attack by hot corrosion and the procedure for inhibiting these forms of attack has been summarized in Figure 9. In general a high chromium content in the alloy has proved to be useful in most cases. Increased Cr and Si levels in the superalloy have led to the inhibition of hot corrosion by the gas phase induced acidic fluxing. Fuel additives such as Mg and Zn in few ppm levels are commonly used in the suppression of attack by V. These form high-melting-point compounds such as magnesium orthovanadate which melts at 1373K. But deposits formed as a result of Mg addition, tend to cause blade fouling[76].

More recently, development of fuel additives to reduce corrosion induced by Na_2SO_4 has occurred and several formulations have been proposed. Addition of chromium to fuel first proposed independently by Condé et al.[77] and Bornstein and Decrescente[78] are now used commercially under the trade-name "Turbogard". It is believed that Cr_2O_3 formed during the combustion process reacts with the oxide ions in Na_2SO_4 and thus reduces the tendency towards basic fluxing[72]. Results of investigation by Deadmore and Lowell[79] have shown that of many additives to fuel including Mg, Ca, Ba, Al, Si, Cr, Fe and Zn, barium was the most effective inhibitor of hot corrosion. However, the use of protective coatings was much more effective in reducing hot corrosion than the fuel additives[80].

4.0 EROSION AND CORROSION

Erosion and corrosion as individual modes of degradation are relatively well understood processes. Their interactions however have not been so extremely studied particularly in relation to high temperature materials and coatings for gas turbine applications[81,82]. Erosive conditions in combination with corrosion are specially undesirable because the reaction product barriers used to develop resistance against corrosion can be destroyed by the erosion process. Studies of oxidation

and erosion of materials including HA-188, MA-754, X-40, IN-738 and aluminized IN-738 have shown that the alumina-formers had lower losses than the chromia-forming alloys[83-86]. This has been demonstrated by Barkalow and Pettit[86] in Figure 10. It has also been shown that pyrolytic carbon and sea salt can cause mechanical erosion of oxide scales[87,88]. The pyrolytic carbon from combustion and ingested sea salt deposited and retained on the surface would of course take part in hot corrosion reactions.

Interaction between erosion and hot corrosion has been studied by various workers and recently reviewed by Galsworthy et al.[89]. Tests at room and higher temperatures (in the range 1023K to 1323K) on oxides formed on nickel, Nimonic alloy 105 and IN-738 with erodants such as SiC, carbon and sea salt over a wide range of particle sizes and velocities have been conducted by Hancock et al.[90,91]. Weight losses were found to be less at higher temperatures possibly due to plasticity of the oxide. Data on the erosion of the superalloys exposed to hot corrosion conditions at 1144K are shown in Figure 11[86]. As observed, the degradation is much more severe in hot corrosion-erosion than in oxidation-erosion. From these studies, the three critical parameters effecting the interaction between corrosion and erosion have been identified as; particulate energy, corrosion product growth rate and the corrosion product toughness and adherence. Excellent examples of turbine blade and NGV failures by corrosion and erosion processes in small helicopter engines have recently been demonstrated[92].

Combined erosion-corrosion processes represent in general more severe degradation than either of these processes acting independently. Procedures to combat combined erosion-corrosion induced degradation are not readily available. The use of filters to prevent particles from entering the engine has been suggested but this has led to a decrease in the engine efficiency and additional maintenance problems[93]. Ceramic coatings may be a means to obtain both resistance to erosion and corrosion. At present, however, dense ceramic coatings which are adherent to the alloy substrate are not available.

5.0 CONCLUSIONS

The effects of alloying elements on the oxidation resistance of superalloys are derived from the oxide stability and alteration in diffusion processes leading to changes in oxide growth rates and plasticity. When present in sufficient amount in the alloy, elements like Al, Cr and Si are technologically important due to the formation of protective oxides such as Al_2O_3, Cr_2O_3 and SiO_2 respectively. The presence of additional reactive elements such as Ce, Y or Hf is known to improve oxide scale adherence. Too low a concentration of Al, Cr or Si is ineffective in providing protection due to preferential internal oxidation of these elements in the alloy.

Purely from an oxidation resistance point of view, Al_2O_3 scales are more efficient than their chromium or silicon counterparts. In aero gas turbines, superalloy components and their coatings where applicable, often incur damage through hot corrosion. This is due to the lack of stability of the oxide layers in the chemically aggressive atmosphere of the hot gases. In this respect, the addition of chromium and/or silicon to the alloy or coating has generally been found to be beneficial, although, the protection mechanism against hot corrosion provided by the addition of silicon is not yet fully understood. Fuel additives such as Cr (in ppm level) have also been proved beneficial. However, much better protection is achieved overall through the use of protective coatings. Corrosion in the presence of erosion can be very aggressive and immediate solutions to this problem are not available. Therefore further research in this field particularly for gas turbine materials and coatings should be very rewarding.

In service alloys forming Al_2O_3 scales such as IN-100 provide good oxidation but they do not in general provide the best overall corrosion resistance when sulfidizing conditions prevail. Alloys such as IN-738 or IN-792 which form Cr_2O_3 scales are superior in this case because of the better performance of Cr_2O_3 scales in the presence of sulfur. In any one application, it is thus important to consider the type of environment in which components or coatings with protective scales are meant to be used. In aero gas turbines this does not only depend on the fuel purity level but also on the

environment in which the engines are operated. In particular, there is strong evidence that the use of aero gas turbines over air polluted industrial regions can be quite detrimental to component lives[94]. Thus from a practical view point it is important that the modes of degradation prevailing in service be fully understood and the rates of damage accumulation fully quantified before any attempts at reducing damage accumulation through the use of protective coatings can be considered. Work is now underway at NAE to document the modes and rates of damage accumulation in aero engine components for several types of engines currently used by the Canadian Forces.

6.0 ACKNOWLEDGEMENTS

This paper was prepared in support of DND-DTHEM "Research and Development Programme on Repair Schemes and Protective Coatings for Aero Engine Components". The author would like to thank Dr. W. Wallace, Head, Structures and Materials Laboratory of NAE-NRCC, for providing him with an opportunity to conduct this work under a NSERC visiting fellowship. The author would also like to acknowledge the support of Drs. W. Wallace and J.-P. Immarigeon for their contribution in the preparation of this document.

7.0 REFERENCES

1. Patnaik, P.C.; Immarigeon, J.-P.; Wallace, W. — *High Temperature Protective Coatings for Aero Gas Turbine Components.* Structures and Materials Laboratory, NAE/NRC, (under preparation) (1985).

2. Patnaik, P.C. — M. Eng. Thesis, McMaster University, Hamilton, Ontario, Canada (1980).

3. Pettit, F.S.; Goward, G.W. — Corrosion Science, 9, 903 (1969).

4. Mrowec, S.; Werber, T. — *Gas Corrosion of Metals.* National Centre for Scientific Information, Warsaw, Poland (1978).

5. Bruckman, A.; Mrowec, S. — Werk, und Korr., 25, 502 (1974).

6. Pettit, F.S. — *Fundamental Aspects of Structural Alloy Designs.* Eds. R.I. Jeffee, B.A. Wilcox, Plenum Press, p. 597 (1976).

7. Hauffe, K. — *Oxidation of Metals.* Plenum Press, N.Y. (1965).

8. Kubaschewski, O.; Hopkins, B.E. — *Oxidation of Metals and Alloys.* Butterworths (London) 1962.

9. Kofstad, P. — *High Temp. Oxidation of Metals.* John Wiley and Sons Inc., New York, p.p. 88, 113 (1966).

10. Peterson, N.L.; Chen, W.K. — *High Temperature Corrosion.* NACE-6, San Diego, p. 101 (1981).

11. Wood, G.W.; Stott, F.H. — *High Temperature Corrosion.* Ref. 10, p. 227 (1981).

12. Smialek, J.L.
Gibala, R.
Reference 10, p. 274 (1981).

13. Kofstad, P.
Lillerud, K.P.
Oxid. of Met., 17, 177 (1982).

14. Hindam, H.
Whittle, D.P.
Oxid. of Met., 18, Nos. 5/6, 245 (1982).

15. Gitzen, W.H., Ed.
Al_2O_3 as a Ceramic Material.
American Ceramic Society Publication, No. 4 (1970).

16. Gallasso, F.S.
Structure and Properties of Inorganic Solids.
International Series in Solid State Physics, 17, (1970).

17. Tien, J.K.
Pettit, F.S.
Metall. Trans. (3), 1587 (1972).

18. Kröger, F.A.
High Temperature Corrosion.
NACE-6, San Diego, Calif., p. 89 (1981).

19. Smeltzer, W.W.
Hindam, H.
Elrefaie, F.A.
High Temperature Corrosion.
Ref. 10, p. 251 (1981).

20. Pfeiffer, H.
Hauffe, K.
Z. Electrochem., 43, 364 (1952).

21. Bastow, B.D.
Wood, G.C.
Whittle, D.P.
Oxid. Met., 16, p. 1 (1981).

22. Hagel, W.C.
Trans. ASM, 56, 583 (1963).

23. Lillerud, K.P.
Kofstad, P.
J. Electrochem. Soc., 127, No. 11, 2397 (1980).

24. Kofstad, P.
Lillerud, K.P.
J. Electrochem. Soc., 127, No. 11, 2410 (1980).

25. Wallwork, G.R.
Hed, A.Z.
Oxid. of Met., 3, No. 2, p. 171 (1971).

26. Wagner, C.
J. Electrochem. Soc., 99, 369 (1952).

27. Wagner, C.
J. Electrochem. Soc., 103, 627 (1956).

28. Wagner, C.
J. Electrochem. Soc., 103, 303 (1956).

29. Wagner, C.
Z. Elektrochem., 63, 772 (1959).

30. Rapp, R.A.
Acta Met., 9, 730 (1961).

31. Rapp, R.A.
Corrosion, 21, 382 (1965).

32. Kirkaldy, J.S.
Oxid. of Metals and Alloys.
ASM, p. 101 (1971).

33. Smeltzer, W.W. — *Defects and Transport in Oxides.* Ed. M.S. Seltzer and R.I. Jaffe, Plenum Press, p. 475 (1973).

34. Smeltzer, W.W.; Whittle, D.P. — J. Electrochem. Soc., 125, No. 7, p. 1161 (1978).

35. Smeltzer, W.W.; Patnaik, P.C. — J. Electrochem. Soc., Vol. 132, No. 5, 1233 (1985).

36. Patnaik, P.C. — Ph. D Thesis, McMaster Univ., Hamilton, Ont. (1984).

37. Stringer, J. — p. 495 in Ref. 33.

38. Elrefaie, F.; Smeltzer, W.W. — J. Electrochem. Soc., 128, p. 2237 (1981).

39. Davies, H.; Smeltzer, W.W. — J. Electrochem. Soc., 121, 543 (1971).

40. Pettit, F.S. — Trans. Metall. Soc. AIME, 239, 1296 (1967).

41. Birks, N.; Rickert, H. — J. Inst. Met., 91, 308 (1963).

42. Whittle, D.P.; Wood, G.C.; Evans, D.J.; Scully, D.B. — Acta Metall., 15, 1747 (1965).

43. Kirkaldy, J.S.; Brown, L.C. — Can. Met. Quart., 2, 89 (1963); 8, 35 (1969).

44. Dalvi, A.D.; Coates, D.E. — Oxid. of Met., 5, 113 (1972).

45. Quets, J.M.; Dresher, W.H. — Journal of Materials, 4, 583 (1969).

46. Giggins, C.S.; Pettit, F.S. — Oxid. of Metals, 14, No. 5, p. 363 (1980).

47. Pettit, F.S.; Goebel, J.A.; Goward, G.W. — Corrosion Science, 9, p. 903 (1969).

48. Birks, N.; Meier, G.H. — *Conference Proceedings, Corrosion-Erosion-Wear of Materials in Emerging Fossil Energy Systems.* NACE-EPRI-LBL, p. 1 (1982).

49. Whittle, D.P.; Stringer, J. — Phil. Trans. Royal Soc., London, A295, p. 309 (1980).

50. Allam, I.M.; Whittle, D.P.; Stringer, J. — Oxid. of Metals, 12, No. 1, 35 (1978).

51. Allam, I.M.
Whittle, D.P.
Stringer, J.
Oxid. of Metals, Vol. 13, No. 4, 381 (1979).

52. Shores, D.A.
High Temperature Corrosion.
NACE-6, San Diego, Calif., p. 493 (1981).

53. Stringer, J.
Ann. Rev. Mat. Sci., 7, p. 477 (1977).

54. Stringer, J.
Proc. of the Symposium on the Properties of High Temperature Alloys.
Eds. Z. Foroulis and F.S. Pettit, Electrochemical Society, New Jersey, p. 513 (1976).

55. Saunders, S.R.J.
Metals Technology, 11, p. 465, Oct. 1984.

56. Corde, J.F.G.
Mcgreath, L.G.
SAE Australasia, 40, Part 6, p. 265 (1980).

57. Pettit, F.S.
Goward, G.W.
Superalloys Source Book, ASM, Metals Park, Ohio, p. 170 (1984).

58. Lewis, H.
Smith, R.A.
Proc. First International Congress on Metallic Corrosion, p. 202 (1965).

59. Donachie, M.J.
Sprague, R.A.
Russell, R.A.
ASTM STP 421, p. 85 (1967).

60. Ryan, K.H.
Kildsig, J.R.
Hamilton, P.E.
WPAFB AMML-TR-67-306, p. 100 (1967).

61. Stetson, A.R.
Moore, V.S.
Proc. Gas Turbine Materials Conf., Naval Ship Eng. Centre, Hyattsville, Maryland, p. 43 (1972).

62. Wheatfall, W.L.
High Temperature Corrosion of Aerospace Alloys.
AGARD-CP-120, p. 237 (1972).

63. Seybolt, A.U.
Corrosion Science, 11, 751 (1971).

64. Davin, A.
Coutsouradis, D.
AGARD-CP-120, p. 222 (1972).

65. Luthra, K.L.
Met. Trans. 13A, 1843, 1853 (1982).

66. Restall, J.E.
AGARD-CP-120, p. 12 (1982).

67. Simons, E.L.
Browing, G.V.
Liebhafsky, H.A.
Corrosion, 11, p. 505t (1955).

68. Decrescente, M.A.
Bornstein, N.S.
Corrosion, 4, 261 (1968).

69. Goebel, J.A.
Pettit, F.S.
Goward, G.W.
Met. Trans. 4A, 261 (1973).

70. Goebel, J.A.
Pettit, F.S.
Goward, G.W.
Deposition and Corrosion in Gas Turbines.
Eds. A.B. Hart and A.J.B. Cutler, Applied Science Purblishers, London, p. 96 (1972).

71. Bornstein, N.S.
Decrescente, M.A.
Roth, H.A.
Proc. of the 1974 Gas Turbine Materials in the Marine Environment, MCIC-75-27, Eds. J.W. Fairbanks and I. Machlin.

72. Bornstein, N.S.
Decrescente, M.A.
Roth, H.A.
Met. Trans., 4A, 1799 (1973).

73. Pettit, F.S.
Private Communication, Univ. of Pittsburgh (USA), March 1985.

74. Baüer, R.
Grünling, H.W.
Schneider, K.
Proceedings of the First Conf. on Advanced Materials for Alternative Fuel Capable Directly Fired Heat Engines, U.S. DOE and EPRI, p. 505 (1979).

75. Giggins, C.S.
Pettit, F.S.
Hot Corrosion Degradation of Metals and Alloys — A Unified Theory.
Pratt and Whitney Aircraft Final Report of AFOSR Contract F44620-76-C-0123 (1979).

76. Lee, S.Y.
Young, W.E.
Vermes, G.
ASME Paper 73-GT-1 (1973).

77. Condé, J. et al.
Proc. 3rd US/UK Navy Conf., "Gas Turbine Materials in a Marine Environment", Bath, Sept. 1976.

78. Bornstein, N.S.
Decrescente, M.A.
In Ref. 77.

79. Deadmore, D.L.
Lowell, C.E.
Report TM-79966, NASA-Lewis Research Centre (1976).

80. Lowell, C.E.
Deadmore, D.L.
Corrosion Science, 18, p. 747 (1978).

81. Tabakoff, W.
Conf. Proc. on Corrosion-Erosion Wear of Materials in Emerging Fossil Energy Systems, Ed. A.V. Levy, An official NACE publication, p. 642 (1982).

82. Toriz, F.S.
Wolverson, J.
Gupta, S.
ASME 85-GT-94.

83. Goebel, J.A.
Spriggs, D.R.
Barkalow, R.H.
Pettit, F.S.
NACE Corrosion, 77 Forum, San Francisco, p. 53/1- (1977).

84. Barkalow, R.H.
Pettit, F.S.
Proceedings of the First Conference on Advanced Materials for Alternative Fuel Capable Directly Fired Heat Engines, Castine, July–August 1974, Eds. J.W. Fairbanks and J. Stringer, p. 270–286.

85. Maasberg, J.A.
Levy, A.V.
Wear, 73, p. 355 (1981).

86. Barkalow, R.H.
Pettit, F.S.
Corrosion/Erosion of Coal Conversion System Materials. (Proc. Conf.), Berkeley, Calif., p. 139 (1979).

87. Restall, J.E.
Inst. of Metallurgists, Series 3, No. 13, Vol. 1, p.p. 4/13–4/26 (1980).

88. Restall, J.E.
Proc. of the 1974 Gas Turbine Materials Conf., Castine, Maine, July 1974, MCIC-75-27, p.p. 195–217.

89. Galsworthy, J.C.
Restall, J.E.
Booth, G.C.
High Temp. Alloys for Gas Turbines. D. Reidel Publishing Company, p. 207 (1982).

90. Hancock, P.
Marie, A.R.I.
Nicholls, J.R.
Proc. of the First Conf. on Advanced Materials for Alternative Fuel Capable Directly Fired Heat Engines, Castine, July–August 1979, Eds. J.W. Fairbanks and J. Stringer.

91. Hancock, P.
Nicholls, J.R.
Proc. of the Second Conf. on Advanced Materials for Alternative Fuel Capable Directly Fired Heat Engines, Monterey, Calif, August 1981.

92. Restall, J.E.
Corrosion-Erosion Behaviour of Materials. Conf. Proceedings, Met. Soc. of AIME, Ed. K. Natesan, p. 209 (1980).

93. Smeltzer, C.E.
Gulden, M.E.
McElmury, S.S.
Compton, W.A.
US Army Aviation Materials Laboratory, Technical Report 70–36 (1970).

94.
The NLR High Temperature Test Facility, NLR Memorandum SM-80-075.

TABLE I

PARABOLIC RATE CONSTANTS* FOR SULFIDATION AND OXIDATION OF SOME BINARY AND TERNARY ALLOYS[5]

Alloy (wt. %)	Temperature K	K_p^*, $g^2cm^{-4}min^{-1}$	
		Sulfidation	Oxidation
Fe-20Cr	1273	5.9×10^{-4}	1.2×10^{-9}
Fe-20Cr	1173	1.1×10^{-4}	1.0×10^{-10}
Ni-20Cr	1273	5.3×10^{-4}	3.0×10^{-9}
Co-20Cr	1073	1.6×10^{-5}	5.0×10^{-11}
Fe-25Cr-5Al	1273	6.5×10^{-5}	1.6×10^{-11}
Ni-20Cr	1073	6.0×10^{-5}	1.2×10^{-10}

*Kp defined as (Weight gain per unit surface area)^2/time

TABLE II

COMPOSITION CF SEA WATER

Constituent	Gms/Litre	%
NaCl	23	52
$MgCl_2 \cdot 6H_2O$	11	25
$Na_2SO_4 \cdot 10H_2O$	8	18
$CaCl_2 \cdot 2H_2O$	1.4	3
KBr, KCl	1.1	2
Total	44.5	100

TABLE III

RELATIVE RANKING ORDER OF OXIDES WHICH LOWER O^{2-} CONTENT OF Na_2SO_4

(CALCULATED AT 1200K)

Oxide	Melting Point K	Reaction	Melting Point of Reaction Product K	PSo_2 for Po_2 = 0.2 atm
Al_2O_3	2313	$Na_2SO_4 + Al_2O_3 = 2NaAlO_2 + SO_2 + 1/2O_2$	2073	$10^{-7.22}$
Cr_2O_3		$2Na_2SO_4 + Cr_2O_3 + 1/2O_2 = 2Na_2CrO_4 + 2SO_2$	1095	$10^{-6.12}$
SiO_2	1993	$Na_2SO_4 + 2SiO_2 = Na_2Si_2O_5 + SO_2 + 1/2O_2$	1147	$10^{-3.36}$
MoO_3	1068	$Na_2SO_4 + MoO_3 = Na_2MoO_4 + SO_2 + 1/2O_2$	960	$10^{-3.29}$
WO_3	1746	$Na_2SO_4 + WO_3 = Na_2WO_4 + SO_2 + 1/2O_2$	971	$10^{-3.2}$
V_2O_5	963	$Na_2SO_4 + V_2O_5 = 2NaVO_3 + SO_2 + 1/2O_2$	903	$10^{-2.28}$
TiO_2	2098	$Na_2SO_4 + 3TiO_2 = Na_2Ti_3O_7 + SO_2 + 1/2O_2$	1401	$10^{+13.73}$

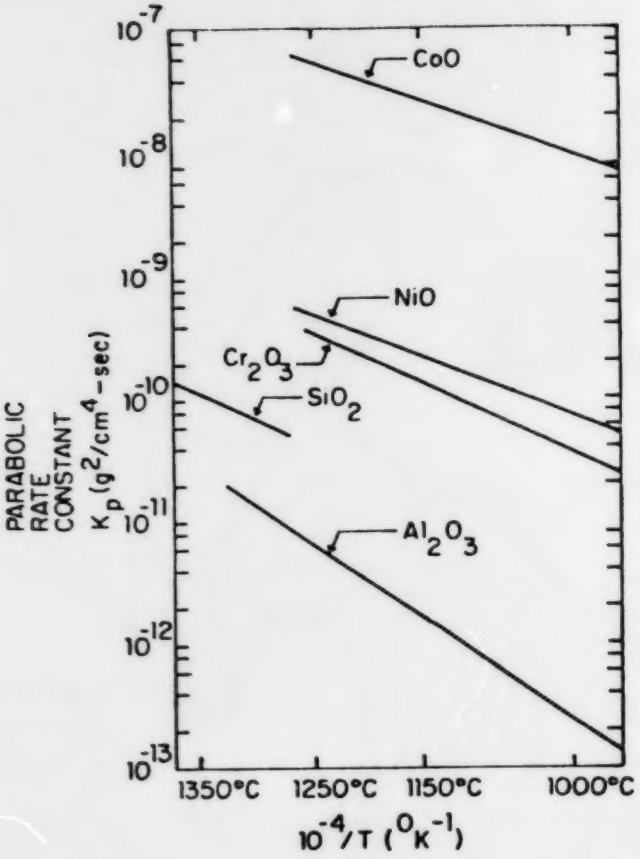

FIG. 1: TEMPERATURE DEPENDENCE OF THE PARABOLIC RATE CONSTANTS FOR THE GROWTH OF VARIOUS OXIDE BARRIERS ON PURE METALS (CoO ON Co, NiO ON Ni, SiO_2 ON Si) AND ALLOYS (Cr_2O_3 ON Ni-30Cr, Al_2O_3 ON Ni-25Al). THE OXIDIZED ENVIRONMENTS WERE 0.1 atm OF O_2 FOR Ni, Ni-30Cr AND Ni-25Al; 0.125 atm OF O_2 FOR Co AND 1 atm OF O_2 FOR Si[5]

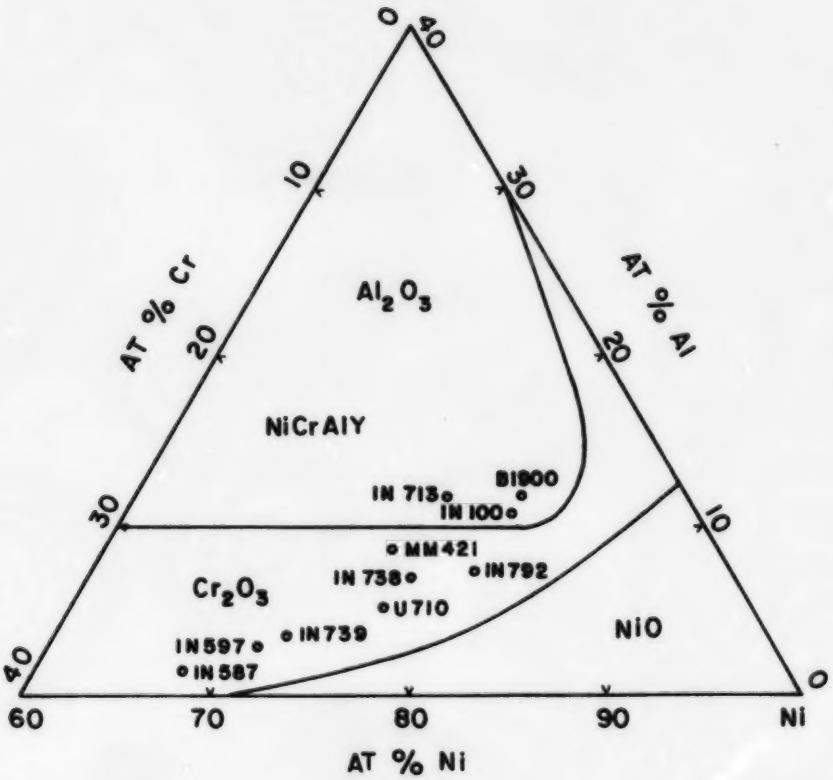

FIG. 2: OXIDE MAP FOR Ni-Cr-Al SYSTEM; SUPERIMPOSED ARE THE TYPICAL Ni BASED SUPERALLOYS AND COATING COMPOSITIONS[14]

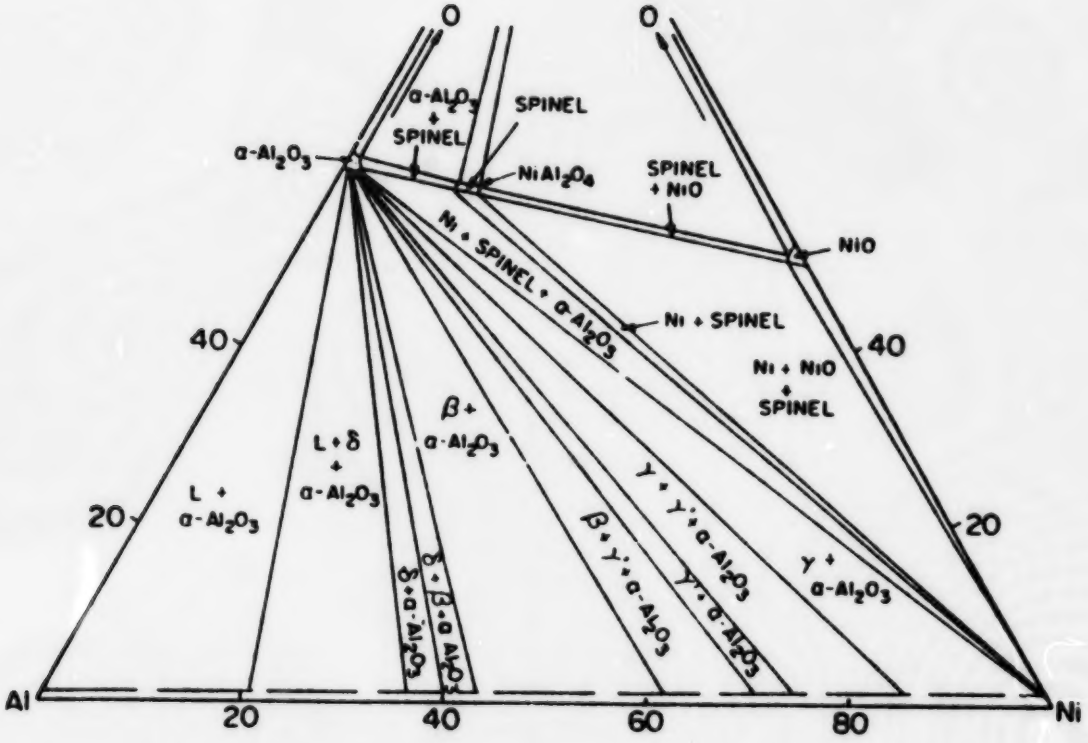

FIG. 3: ISOTHERMAL SECTION AT 1273K IN THE Ni-Al-O PHASE DIAGRAM[38]

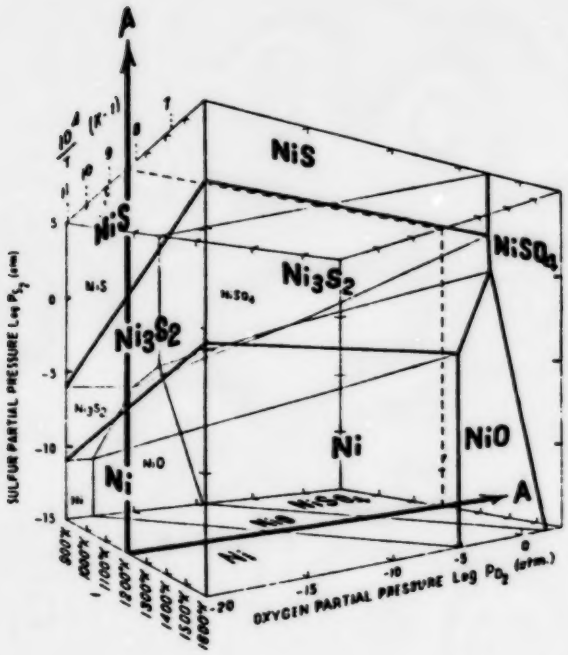

FIG. 4: STABILITY DIAGRAM FOR Ni-S-O SYSTEM AS A FUNCTION OF TEMPERATURE (900-1600K). SECTION A-A SHOWN IN FIG. 5[45]

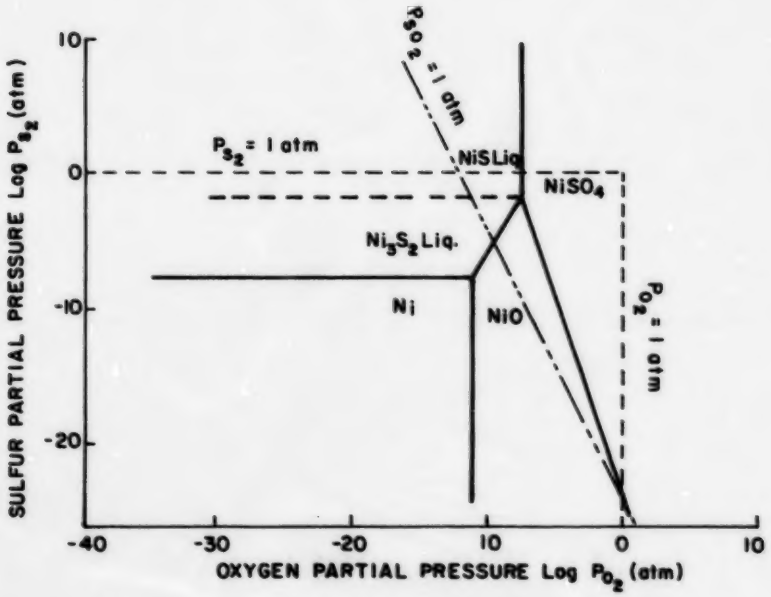

FIG. 5: STABILITY DIAGRAM FOR Ni-S-O AT 1200K (SECTION A-A FROM FIG. 4)

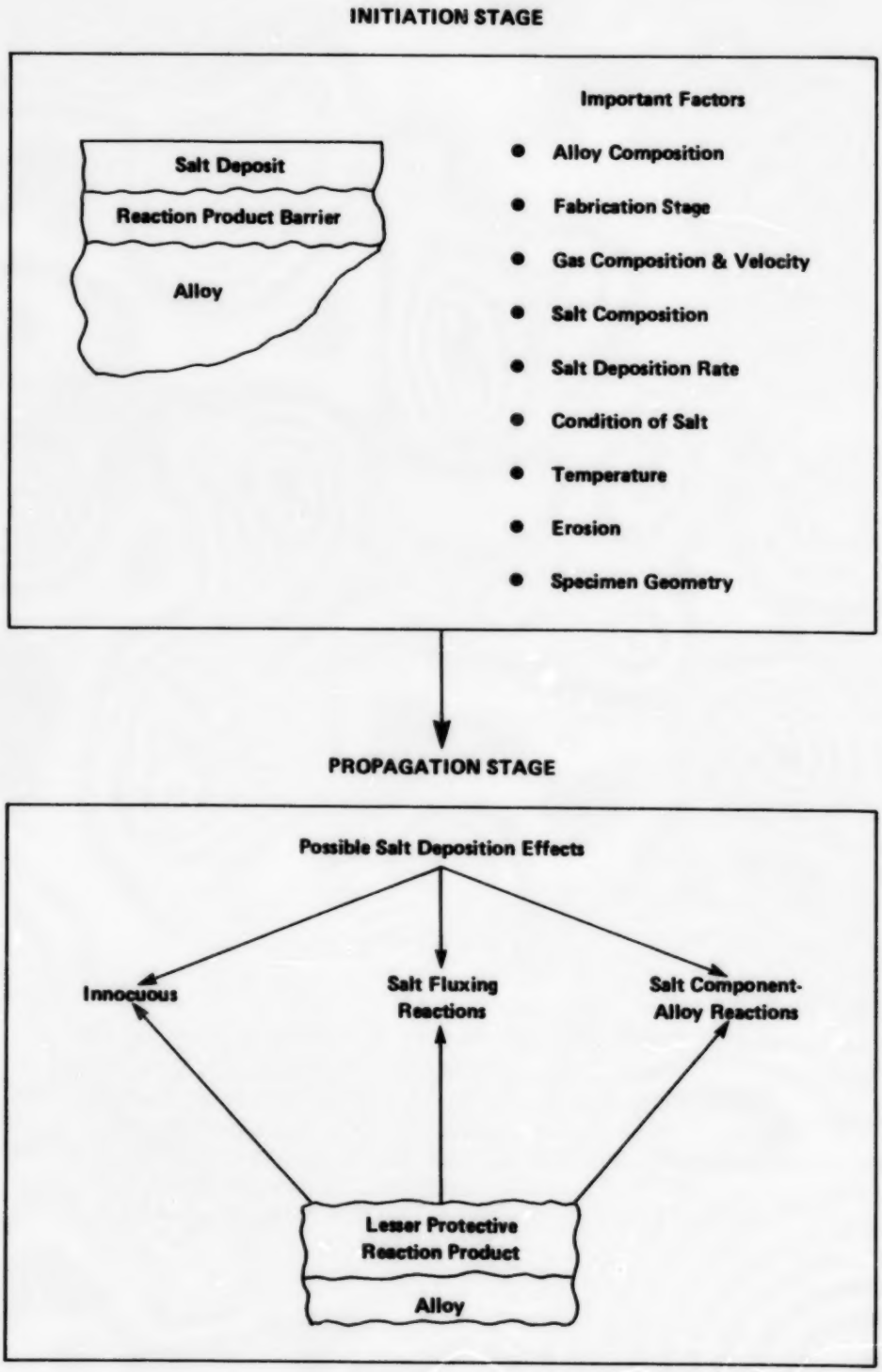

FIG. 6: HOT CORROSION CRONOLOGY[57]

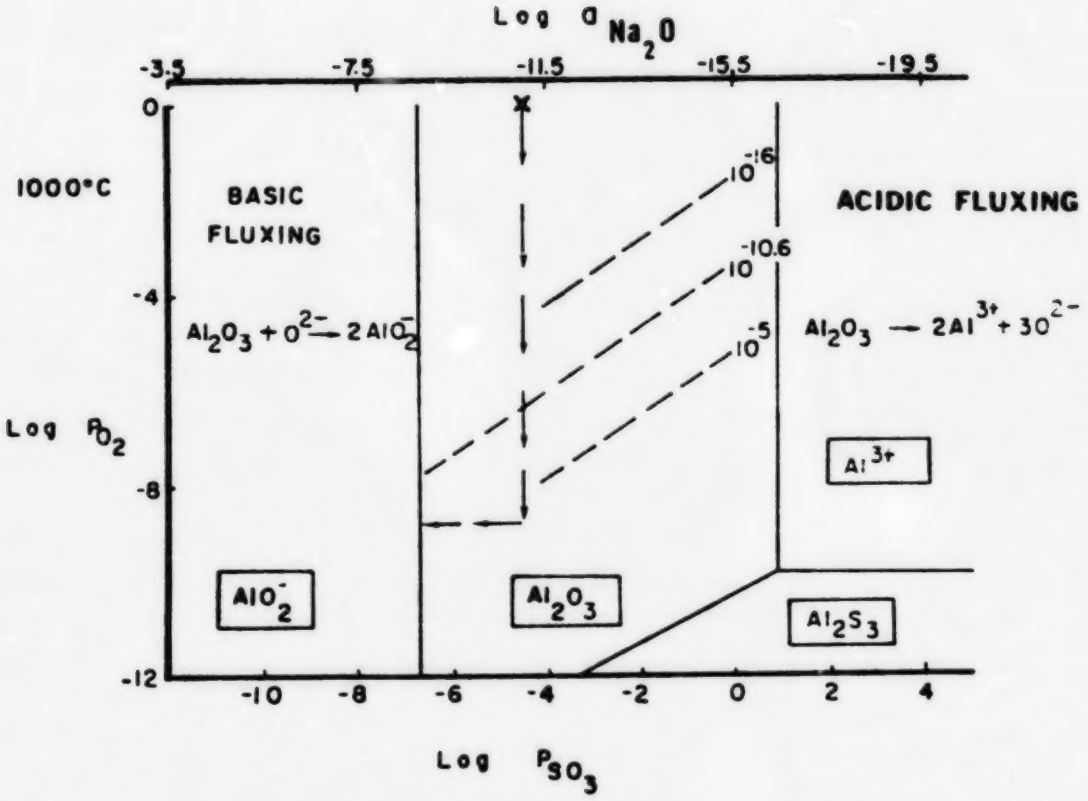

FIG. 7: STABILITY DIAGRAM[69] SHOWING THE PHASES OF ALUMINUM THAT ARE STABLE IN Na_2SO_4 AT 1273K. THE ARROWS SHOW HOW THE COMPOSITION CAN CHANGE BECAUSE OF REMOVAL OF OXYGEN AND SULFUR. THE DASHED LINES ARE SULFUR ISOBARS AND THE ISOBAR OF $10^{-10.6}$ IS THE SULFUR PRESSURE AT WHICH Al_2S_3 CAN BE FORMED BENEATH AN EXTERNAL Al_2O_3 SCALE ON Ni-31Al

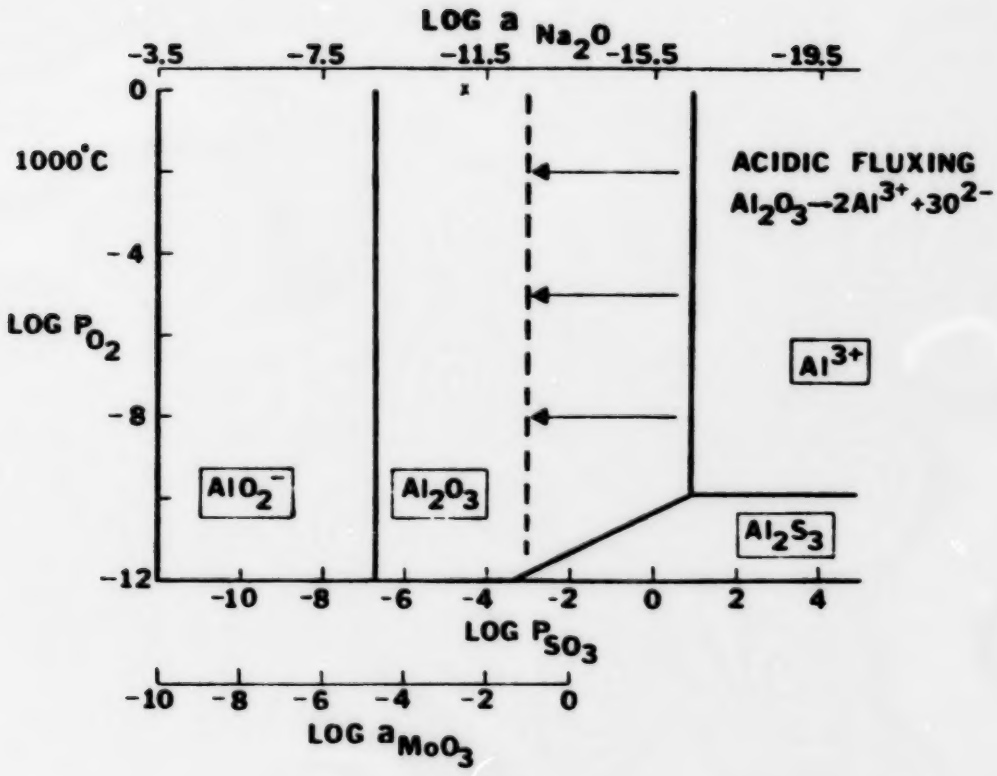

FIG. 8: STABILITY DIAGRAM SHOWING THE DISPLACEMENT OF THE BOUNDARY (ARROWS) AT WHICH ACIDIC FLUXING OF Al_2O_3 CAN OCCUR FOR THE CASE WHERE Na_2SO_4 CONTAINS MoO_3 IN SOLUTION AT AN ACTIVITY OF MoO_3 = 0.1, T = 1273K[70]

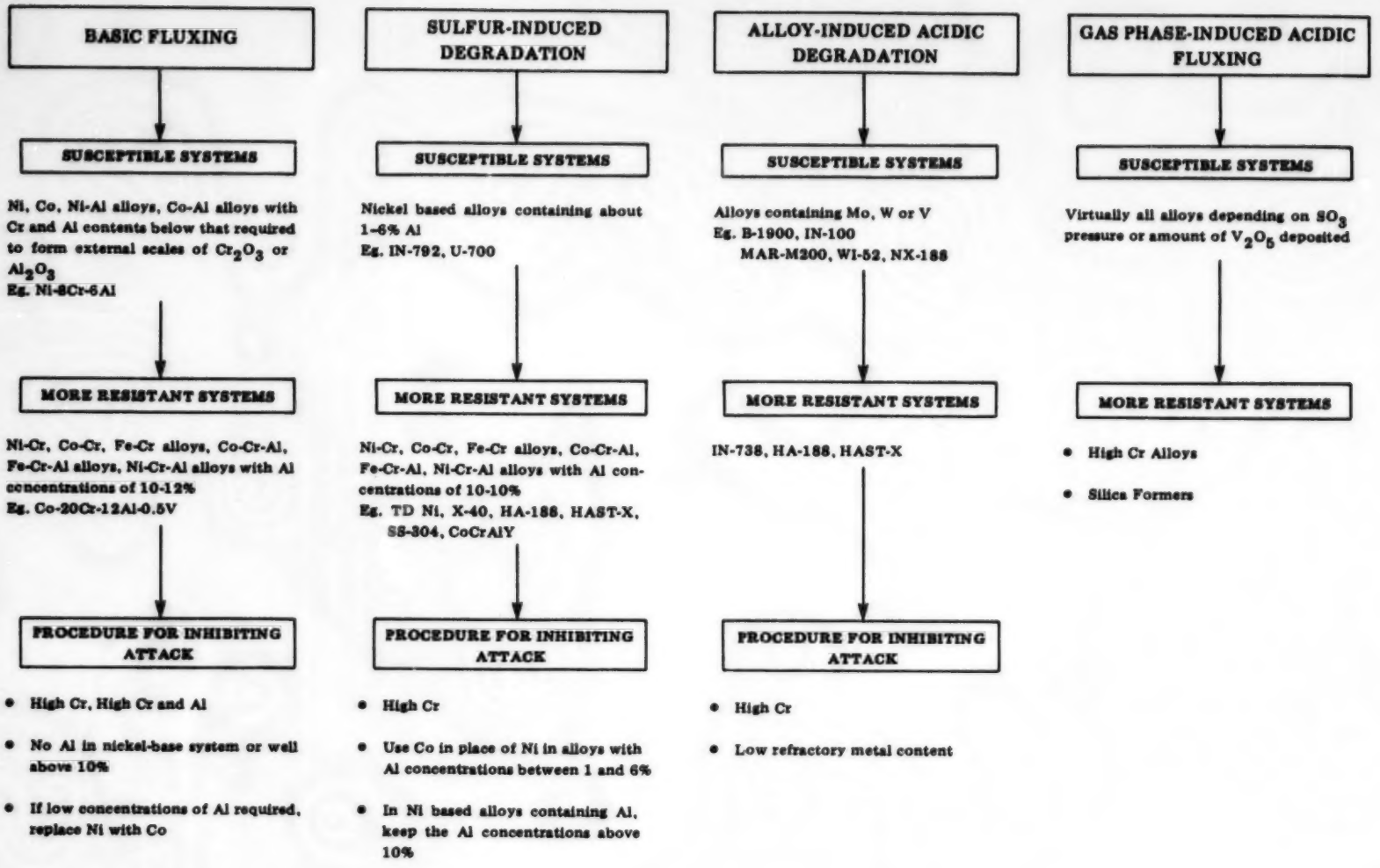
BASIC FLUXING
SUSCEPTIBLE SYSTEMS
Ni, Co, Ni-Al alloys, Co-Al alloys with Cr and Al contents below that required to form external scales of Cr_2O_3 or Al_2O_3
Eg. Ni-8Cr-6Al
MORE RESISTANT SYSTEMS
Ni-Cr, Co-Cr, Fe-Cr alloys, Co-Cr-Al, Fe-Cr-Al alloys, Ni-Cr-Al alloys with Al concentrations of 10-12%
Eg. Co-20Cr-12Al-0.5V
PROCEDURE FOR INHIBITING ATTACK
• High Cr, High Cr and Al
• No Al in nickel-base system or well above 10%
• If low concentrations of Al required, replace Ni with Co
SULFUR-INDUCED DEGRADATION
SUSCEPTIBLE SYSTEMS
Nickel based alloys containing about 1-6% Al
Eg. IN-792, U-700
MORE RESISTANT SYSTEMS
Ni-Cr, Co-Cr, Fe-Cr alloys, Co-Cr-Al, Fe-Cr-Al, Ni-Cr-Al alloys with Al concentrations of 10-10%
Eg. TD Ni, X-40, HA-188, HAST-X, SS-304, CoCrAlY
PROCEDURE FOR INHIBITING ATTACK
• High Cr
• Use Co in place of Ni in alloys with Al concentrations between 1 and 6%
• In Ni based alloys containing Al, keep the Al concentrations above 10%
ALLOY-INDUCED ACIDIC DEGRADATION
SUSCEPTIBLE SYSTEMS
Alloys containing Mo, W or V
Eg. B-1900, IN-100
MAR-M200, WI-52, NX-188
MORE RESISTANT SYSTEMS
IN-738, HA-188, HAST-X
PROCEDURE FOR INHIBITING ATTACK
• High Cr
• Low refractory metal content
GAS PHASE-INDUCED ACIDIC FLUXING
SUSCEPTIBLE SYSTEMS
Virtually all alloys depending on SO_3 pressure or amount of V_2O_5 deposited
MORE RESISTANT SYSTEMS
• High Cr Alloys
• Silica Formers

FIG. 9: ALLOY SYSTEMS SUSCEPTIBLE TO ATTACK BY HOT CORROSION AND PROCEDURES TO INHIBIT SUCH DEGRADATION[57]

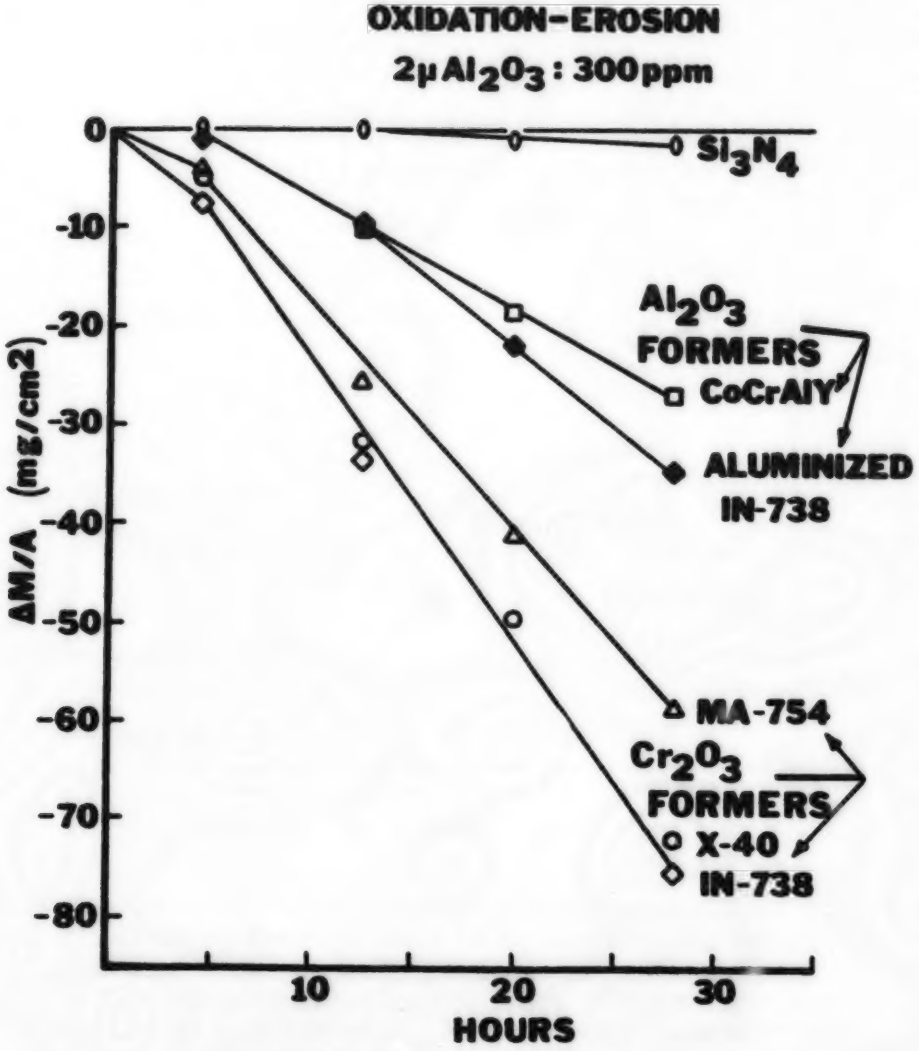

FIG. 10: KINETICS DATA FROM THE TESTING OF MATERIALS AT 1144K IN THE OXIDATION-EROSION TEST USING 2 μm Al_2O_3 PARTICLES AT A LOADING OF 300 ppm IN A BURNER RIG[86]

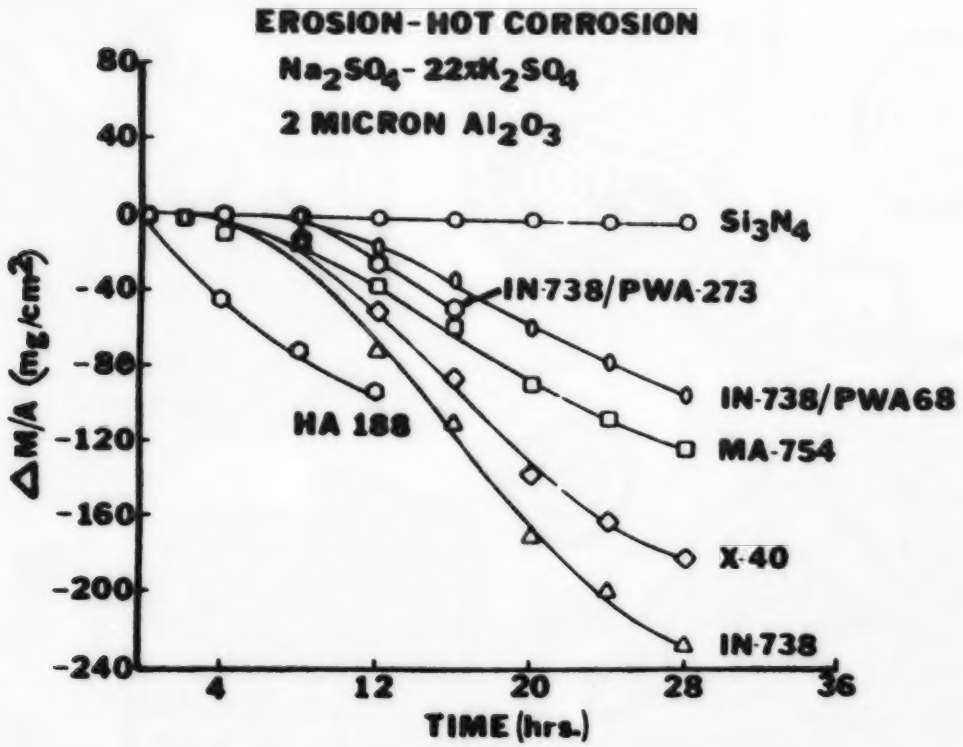

FIG. 11: KINETICS DATA FOR MATERIALS EXPOSED TO EROSION-HOT CORROSION CONDITIONS AT 1144K WITH A RATE OF SALT INGESTION 0.05 mg/cm^2-hr. Na_2SO_4-22% K_2SO_4 USING 2 μm Al_2O_3 IN A BURNER RIG[86]. PWA 273 IS AN ALUMINIDE COATING BY PACK CEMENTATION PROCESS WHEREAS PWA 68 IS AN OVERLAY Co-25Cr-6Al-0.2Y COATING

REPORT DOCUMENTATION PAGE / PAGE DE DOCUMENTATION DE RAPPORT

REPORT/RAPPORT	REPORT/RAPPORT
NAE-AN-33	NRC No. 25075
1a	1b

REPORT SECURITY CLASSIFICATION CLASSIFICATION DE SÉCURITÉ DE RAPPORT	DISTRIBUTION (LIMITATIONS)
Unclassified	Unlimited
2	3

TITLE/SUBTITLE/TITRE/SOUS-TITRE

High Temperature Oxidation and Hot Corrosion of Nickel and Cobalt Based Superalloys

4

AUTHOR(S)/AUTEUR(S)

P.C. Patnaik

5

SERIES/SÉRIE

Aeronautical Note

6

CORPORATE AUTHOR/PERFORMING AGENCY/AUTEUR D'ENTREPRISE/AGENCE D'EXÉCUTION

National Research Council Canada
National Aeronautical Establishment — Structures and Materials Laboratory

7

SPONSORING AGENCY/AGENCE DE SUBVENTION

8

DATE	FILE/DOSSIER	LAB. ORDER COMMANDE DU LAB.	PAGES	FIGS/DIAGRAMMES
85-10			35	11
9	10	11	12a	12b

NOTES

13

DESCRIPTORS (KEY WORDS)/MOTS-CLÉS

1. Superalloys — Corrosion
2. Superalloys — Oxidation
3. Nickel Alloys — Corrosion
4. Nickel Alloys — Oxidation
5. Cobalt Alloys — Corrosion
6. Cobalt Alloys — Oxidation

14

SUMMARY/SOMMAIRE

Oxidation and hot corrosion are often the two most important modes of degradation that superalloys undergo in a high temperature gas turbine atmosphere. In general, the corrosion resistance of superalloys has been sacrificed to achieve adequate high temperature strength. Therefore turbine blade and vane materials are often protected from these modes of degradation by the use of protective coatings. Three classes of coating materials based on aluminizing, chromizing and more recently siliconizing treatments are usually considered due to their resistance to oxidation, sulfidation (hot corrosion) processes.

The purpose of this paper is to review the oxidation and hot corrosion properties of superalloys and coating materials of relevance to aero gas turbine engine hot-section, with particular emphasis on the interaction between gas phase or molten salt deposits and the substrate alloy/coating system. The recent theories on these processes are reviewed. Finally, the effects of erosion on the corrosion properties of superalloys and coatings are also discussed.

15